Journal of Research and Applications in Mechanical Engineering
ISSN: 2229-2152 (Print); 2697-424x (Online)
(2025) Vol. 13, No. 2, Paper No. JRAME 25-13-023
[DOI: 10.14456/jrame.2025.23]

Research Article

Numerical Study of Anthracite Blended with Petroleum Coke on Swirl-JET Burner in Cement Kiln

A. Kaewpradap[1,*]
J. Charoensuk[2]
C. Chantang[1]
[1] *Department of Mechanical Engineering, King Mongkut's University of Technology Thonburi, Bangkok 10140, Thailand*
[2] *Department of Mechanical Engineering, Faculty of Engineering, King Mongkut's Institute of Technology Ladkrabang, Bangkok 10520, Thailand*

Received 31 August 2024
Revised 5 November 2024
Accepted 7 November 2024

Abstract:
This research focuses on studying and improving the combustion of anthracite coal blended with Petroleum coke in a ratio of 89:11 by mass. The numerical study was conducted using Ansys Fluent. In cement kiln operations, the Swirl-JET burner has been observed to cause melting of cement at the burner outlet, leading to clogging after a few months of operation. To validate the numerical model with real operating conditions of the cement kiln burner, the study analysed char particle combustion, combustion characteristics, kiln surface temperature, air velocity distributions, and temperature distribution. Additionally, the research examined the effect of varying the swirl angle of the swirl air outlet (40°, 25° and 14°). The results showed that decreasing the swirl angle reduced coal scattering at the burner outlet and shifted combustion further from the burner outlet. Furthermore, blending Anthracite coal with Petroleum coke in a ratio of 89:11 by mass, due to the smaller particle size and higher lower heating value, improved combustion characteristics. This blend prevented recirculation flow near the burner outlet and enhanced flame temperature along the cement kiln. In conclusion, decreasing the swirl angle and blending Anthracite coal with Petroleum coke are effective strategies to reduce burner clogging and improve flame temperature in cement kiln operations.

Keywords: *Blended coal, Cement Kiln, Cement-JET Burner, Petroleum coke, Swirl angle*

1. Introduction

The rotary kiln is a crucial of equipment in the production of various products in the cement industry. Data from a cement plant indicates that the burner installed in the rotary kiln often experiences significant raw meal buildup, leading to burner blockages within just 2 to 3 months of operation. This frequent blockage necessitates plant shutdowns for maintenance, impacting production targets. Consequently, there has been an effort to find methods to reduce burner blockages. However, actual experimentation with operational rotary kilns poses risks to both personnel and product quality and involves high costs. Therefore, preliminary studies using mathematical modeling were conducted to identify the suitable approaches before practical implementation.

Mastorakos et al. [1] and Wang et al. [2] presented a CFD model of cement kilns for predicting flame characteristics, heat transfer, and clinker chemistry. Mingyue et al. [3] and Granados et al. [4] explored the use of oxidant air, which has a higher oxygen concentration than normal, to enhance flame temperature and combustion efficiency. Mouratidis et al. [5] developed a mathematical model for cement kiln combustion, aiming to minimize computational resources. Bhad et al. [6] investigated the effects of adjusting the swirl angle, finding that reducing the swirl angle helps to

* Corresponding author: A. Kaewpradap
E-mail address: amornrat.kaw@kmutt.ac.th

concentrate and reduce the combustion zone size. Mujumdar and Ranade [7] presented a CFD model of cement kilns that predicts performance, including heat sink settings. Mikulčić et al. [8,9] introduced a CFD model of cement kilns with a focus on designing and optimizing calciners to reduce CO2 emissions. Ariyaratne et al. [10] and Ma et al. [11] examined the impact of particle size, injection location, fixed carbon content of coal, and swirl angle on combustion efficiency in cement kilns. Cecílio et al. [12] and Alcaide-Morenoa et al. [13] investigated the effects of increasing secondary air on combustion efficiency, finding that it enhances performance. Ngadi and Lahlaouti [14] developed a 2D CFD model of a cement kiln using petroleum coke and olive pomace (OP) as fuel, employing the standard K-ϵ model for simulation. Elattar et al. [15] explored the effects of swirl angle, primary air flow rate, and secondary air temperature on combustion. Elattar [16] studied the impacts of primary air ratio, fuel jet momentum, and energy on peak kiln flame temperature and wall temperatures. However, burner blockages, often due to suboptimal combustion conditions, present significant challenges that lead to operational inefficiencies and increased maintenance costs. Consequently, this study is to address the burner blockage by modifying combustion parameters and fuel composition. The mathematical model of burner is developed for solving the problem of burner blockage in coal combustion in cement kilns by reducing the swirl angle and altering the coal properties to include anthracite coal mixed with petroleum coke. The analysis will focus on trends in particle char mass fraction exiting the burner, oxygen mass fraction at the kiln outlet, and the surface temperature profile of the kiln wall. Addressing blockage issues in cement kiln burners offers key benefits, including extending the operational lifespan of the burner and reducing the frequency of plant downtime for maintenance. These improvements positively impact overall production efficiency by allowing for more continuous operation and minimizing interruptions.

2. Methodology

2.1 Process description

Operational data of the cement kiln from available cement plant shows that thermal energy for cement production comes from burning anthracite pulverized coal in a multichannel swirl-jet burner at the kiln inlet. The primary air injected through the burner averages 23°C, while the secondary air, flowing between the kiln wall and the burner, averages around 1000 °C. Key parameters for assessing combustion characteristics include the temperature of the kiln's external wall along its length and the oxygen concentration at the kiln outlet. Different kiln sections are insulated with various materials, and the effects of kiln wall temperature and burner position are shown in Figure 1.

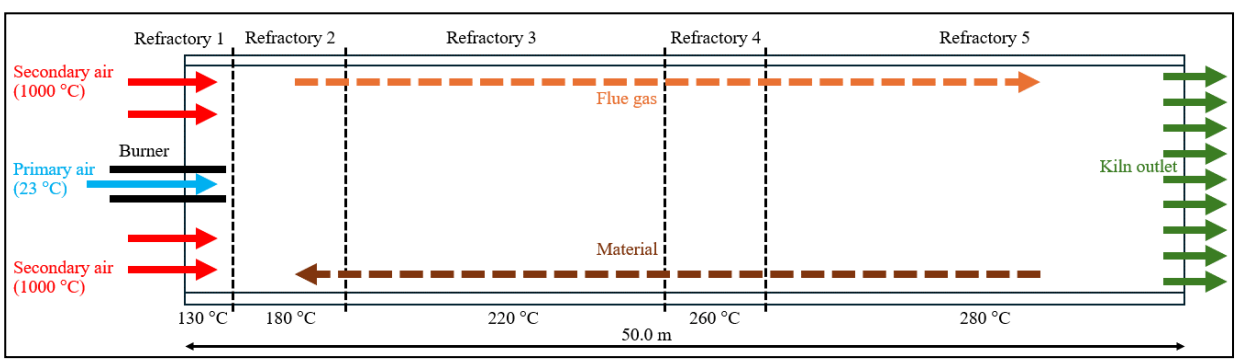

Fig. 1. The operational process of a cement kiln from available cement plant

Table 1: The length of the refractory zones and the outer kiln surface temperature range of each refractory zone.

Refractory zone	1	2	3	4	5
Range (m)	0 - 2	2 - 10	10 - 23	23 - 31	31 - 50
Outer kiln Surface temp. (°C)	120 - 140	160 - 220	200 - 240	240 - 280	260 - 300

2.2 Anthracite coal

Anthracite coal is the highest rank of coal. It is a hard, brittle, and black lustrous coal, often referred to as hard coal, containing a high percentage of fixed carbon and a low percentage of volatile matter.

2.3 Petroleum coke (Pet-coke)

Petroleum coke is a hard, black or dark gray solid with a metallic luster and porosity. It consists of carbon, with tiny graphite crystals forming granules, columns, or needles. Its composition includes 90-97% carbon, 1.5-8% hydrogen, and traces of nitrogen, chlorine, and sulfur.

2.4 Swirl number

The swirl number quantifies the intensity of fluid swirling within a flow. A higher swirl number indicates a greater degree of swirl in the fluid, and it can be calculated using the following equation [17].

$$SN = \left(\frac{2}{3}\right)\frac{1-(D_{hub}/D_{sw})^3}{1-(D_{hub}/D_{sw})^2}tan\theta \quad (1)$$

Where SN is swirl number

D_{hub} is swirler hub diameter (similar to a bluff-body)

D_{sw} is swirler diameter

θ is flat vanes angles

3. Simulation

In the current study, the kiln referenced is from an operational plant, and the simulation was conducted using ANSYS Fluent 2023 R1. To verify the accuracy of the study, the actual operating conditions of the cement kiln burner provided by the plant were used to set up the mathematical model. The accuracy of the mathematical model was validated by comparing the temperature of the outer wall surface of the kiln and the oxygen content at the kiln outlet.

3.1 Simulation parameters

The study will proceed as follows: The first step involves verifying the accuracy of the mathematical model for the combustion of anthracite coal. The next step examines the impact of adjusting the swirler angles. Following this, the study investigates the influence of modifying coal properties by blending anthracite coal with petroleum coke to enhance combustion efficiency. Finally, the study explores the combined influence of blended coal properties and swirl air inlet angles. It was found that when switching to fuels with increased low heating value, a higher air supply for combustion is required. However, to maintain similar airflow characteristics, the primary air volume is kept constant, with the excess air being directed exclusively to the secondary air, as shown in Table 2.

Table 2: Show the various parameters used in the simulation of anthracite coal combustion.

Parameters	**Value**	**Temperature (°C)**
Swirl air (kg/s)	0.5960	23
Coal carrier air (kg/s)	0.4430	23
Jet air (kg/s)	0.4447	23
Axial air (kg/s)	0.3735	23
Secondary air (kg/s)	8.9043	1000
Secondary air (blended coal) (kg/s)	9.2705	1000
Equivalence ratio	0.9091	-
Swirler angle (Degree)	14°/ 25°/40°	-
Swirl number	0.24/0.45/0.81	-
Coal Feed rate (kg/s)	1.389	-
Physical properties of coal	Anthracite coal	Blended Anthracite coal with Petroleum coke
Low heating value (kJ/kg)	20543.44	21190.66
Fixed carbon (%)	41.16	46.20
Volatile content (%)	22.77	18.54
Min. Particle dia. (μm)	1.8	1.8
Max. Particle dia. (μm)	122	72
Mean Particle dia. (μm)	17.6	11.44
No. of Size fraction	10	10
Rosin Rammler spread parameter	0.93	0.942

3.2 Simulation burner model

The 3D model used in this study is 30 meters instead of 50 meters long and was constructed as a 1-quadrant model to allow for periodic modeling, which helps decrease computational resources. The position of the burner outlet is shown in Figure 2. Swirl air flows through the swirler located in the center of the burner, and it is directed to exit at an angle to the model's axis, creating the desired swirl effect. The coal carrier air, located next to the swirl air outlet, flows straight out along with the pulverized coal used for combustion. Axial air is released from the outermost annular jet surrounding the burner, while the jet air exits through holes arranged in a circular pattern between the coal carrier air and axial air outlets. This jet air flows out rapidly, and secondary air enters the kiln through the large gap between the burner wall and the inner wall of the kiln. In the meshing process, a tetrahedral mesh is used. At the interface between the fluid domain and the solid domain, which is the inner wall of the kiln, five inflation layers are created to reduce calculation errors in the near-wall region. The total number of mesh elements is approximately 450,000, as shown in Figure 3. This is the finest mesh that the tools could calculate within a reasonable time frame. In models with fewer mesh elements, floating-point errors occurred, preventing the calculations from being completed.

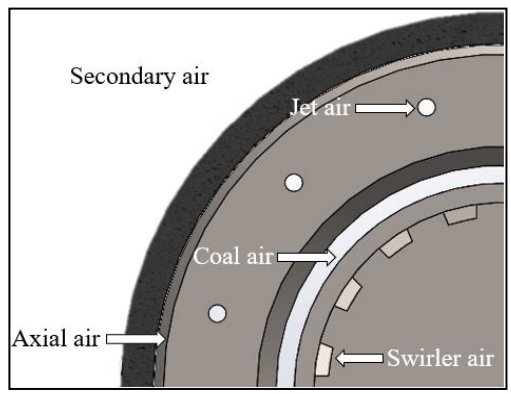

Fig. 2. Burner model

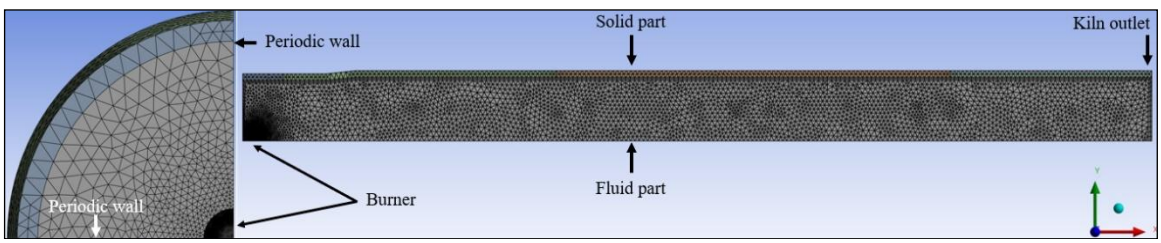

Fig. 3. Mesh details of 3-D model

Table 3: Show the mesh independent test of the simulation model.

Approximately Mesh elements (elements)	%Error (%)	Time used (Hour)
150,000	Floating-point error	-
240,000	Floating-point error	-
350,000	Floating-point error	-
450,000	11.67	20.0

3.3 Boundary conditions

The calculations employed a steady-state approach, using the Standard k-ε model for viscosity and the Discrete Ordinates (DO) model for radiation. Coal combustion was modeled using species transport. All inlets were treated as mass flow inlets with flow direction normal to the boundary, except for the swirl air, where the flow angle was adjusted. Coal injection was modeled as combusting particles at the coal carrier air inlet boundary. A volumetric heat sink was configured at the fluid-solid interface to absorb heat from combustion. The first-order upwind scheme was applied to all governing equations. The effects of kiln rotation and gravity were not considered in this calculation.

4. Results and Discussion

4.1 Simulation results of Anthracite combustion with 40 ° swirl angle (base case)

The simulation shows that char mass fraction peaks near the burner outlet and rapidly burner near the burner due to swirl air dispersing the char around the burner (Figure 4). This aligns with high velocity vectors and strong secondary air induction, creating a vortex flow near the burner, which cause of rapidly combustion (Figure 5). Before combustion, oxygen mass fraction is high (indicated by the red region) but quickly depletes during the process. The with oxygen content at the end of the kiln measuring around 2.59% (Figure 6). The temperature rise across the kiln's cross-section from the inlet, consistent with oxygen mass fraction results, as oxygen is quickly consumed upon pulverized coal contact (Figure 7). The coal combustion model's outer kiln surface temperature profile (Figure 8) matches actual conditions shown in Table 1. The surface temperature starts at about 120°C in the first 4 meters, rising quickly to 220°C-240°C over the next 25 meters, and then increasing to around 260°C. This profile aligns with operational data, despite actual temperatures fluctuating between 200°C and 260°C. Thus, the model is deemed reliable for further calculations blended coal combustion and adjusting the swirler angle.

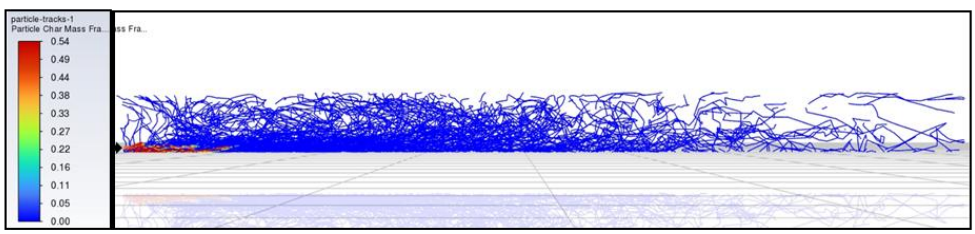

Fig. 4. Particle char mass fraction from the coal combustion model in the cement kiln

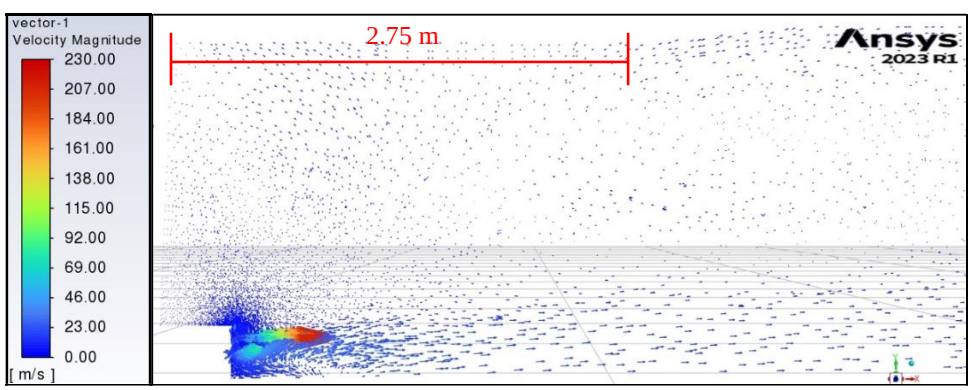

Fig. 5. Velocity vectors of the mixture from the coal combustion model in the cement kiln

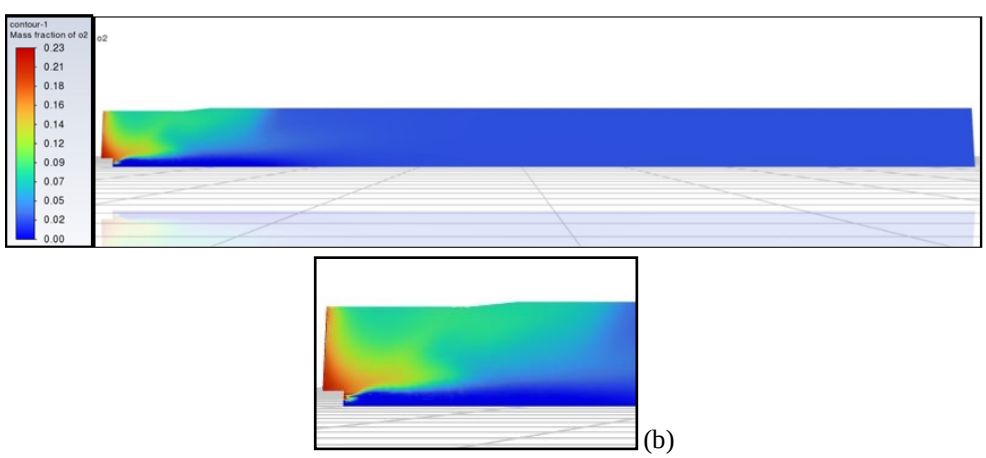

Fig. 6. Oxygen mass fraction from the coal combustion model (a) in the cement kiln and (b) near burner zone.

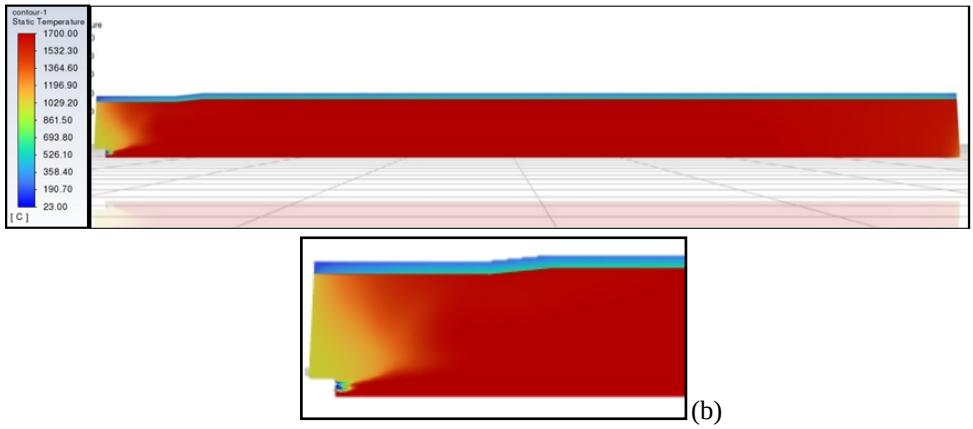

Fig. 7. Temperature distribution from the coal combustion model (a) in the cement kiln and (b) near burner zone.

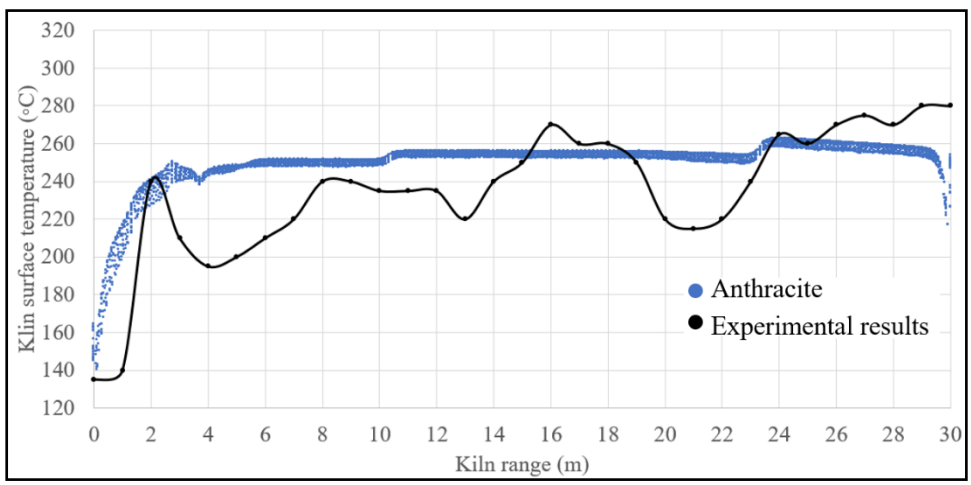

Fig. 8. Outer kiln surface temperature from the coal combustion model.

4.2 Simulation results of Anthracite combustion with difference swirl angle (14°, 25° and 40°)

The effects of swirl angle variation on combustion. When the swirl angle was lower, the swirl flow decreased and affected the lower char mass fraction due to the shifted and delayed combustion. Figure 9 indicates that reducing the swirl angle (40° to 14°) extends the burn-out distance of pulverized coal beyond the reference angle of 40°, while also reducing the dispersion of pulverized coal near the burner exit. This is consistent with the velocity vectors of the mixture at the burner exit, where reducing the swirl angle alleviates the issue of pulverized coal dispersion and recirculation near the burner exit, thereby increasing the forward momentum of the air and coal flow (Figure 10). For the oxygen mass fraction, a reduction in the swirl angle results in an extended burn-out distance, indicating that combustion occurs further from the burner exit, with oxygen levels at the model exit measured at 2.59%, 2.58% and 2.56% for swirl angles of 40°, 25° and 14°, respectively (Figure 11). The reasons were the adjusting the swirl angle modified the trajectory and distribution of the airflow and pulverized coal within the burner. This affects how air and coal particles interact, potentially optimizing the mixing and combustion process. A reduced swirl angle can lead to a more direct flow, minimizing recirculation zones that contribute to particle buildup and blockage. The temperature distribution in the kiln shows that lowering the swirl angle shifts the high-temperature combustion zone further from the burner exit (Figure 12). Additionally, the kiln surface temperature study reveals that between 0 to 5 meters, the high-temperature region extends further when the swirl air angle is reduced. During 18-30 metes, the outer kiln surface temperature decreases more rapidly with lower swirl angles, suggesting reduced flame dispersion and less heat transfer to the kiln wall (Figure 13).

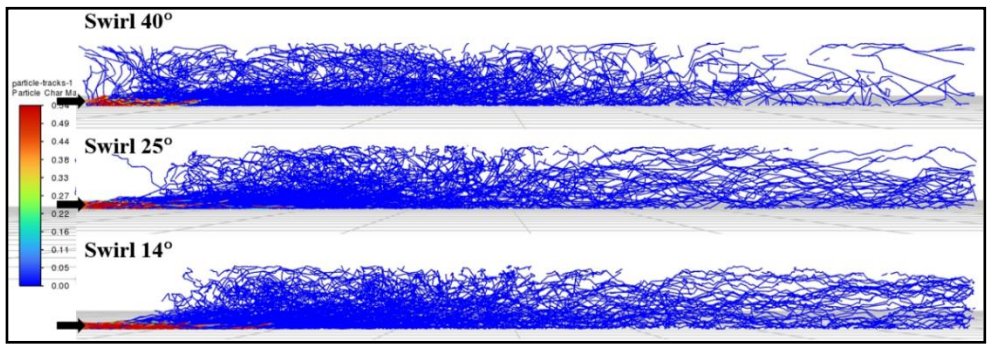

Fig. 9. Particle Char Mass Fraction from the coal combustion model at different swirler angles.

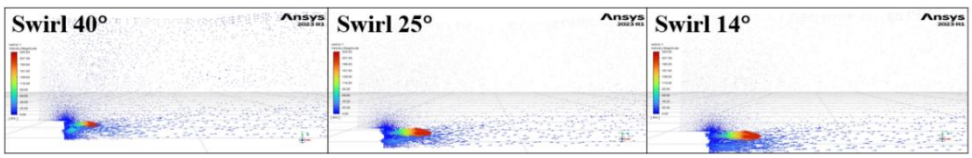

Fig. 10. Velocity vectors from the coal combustion model at different swirler angles.

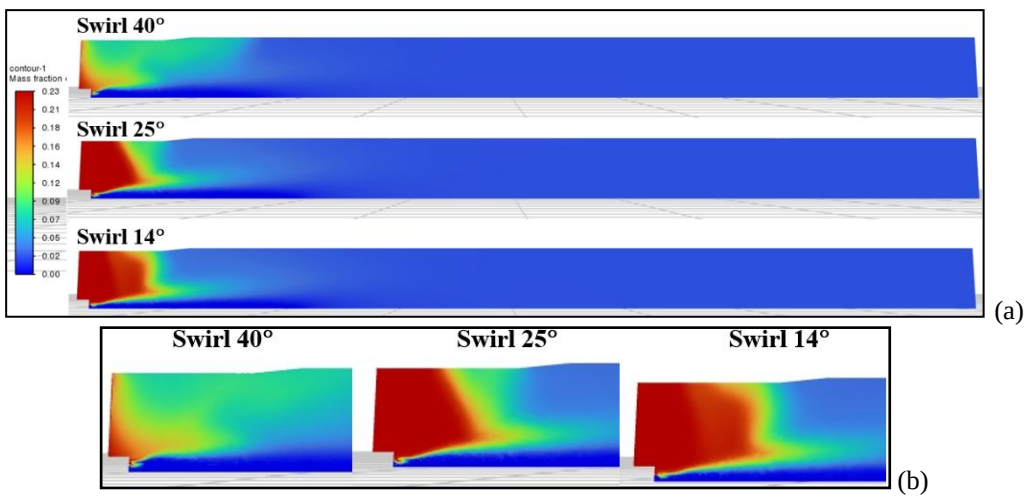

(a)

(b)

Fig. 11. Oxygen mass fraction from the coal combustion model (a) at different swirler angles (b) near burner zone

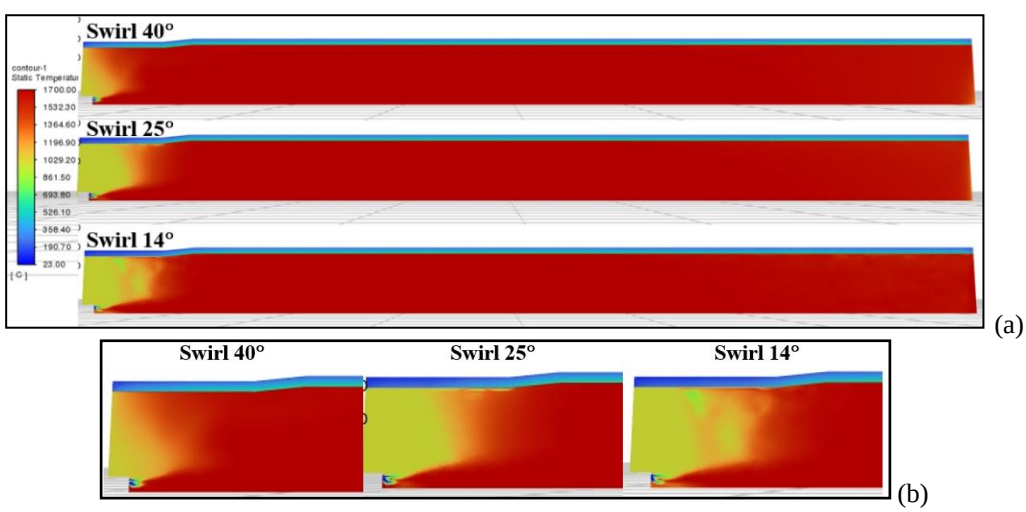

(a)

(b)

Fig. 12. Temperature distribution from the coal combustion model (a) different swirler angles (b) near burner zone.

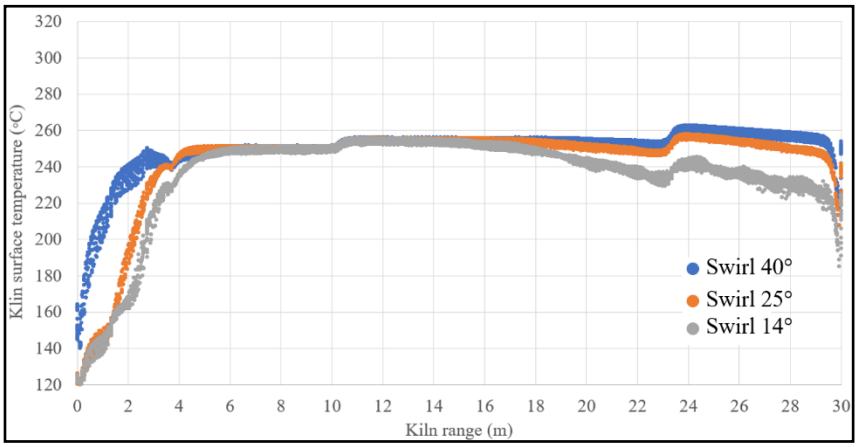

Fig. 13. Outer kiln surface temperature from the coal combustion model at different swirler angles

4.3 Simulation results of Anthracite combustion blended with petroleum coke with 40 ° swirl angle.

The simulation study indicates that the mass of the blended coal exhibits a longer combustion distance compared to pure anthracite coal and does not disperse near the burner exit (Figure 14). This observation aligns with the velocity vectors of the mixture exiting the burner, where no recirculation flow was detected at the burner outlet (Figure 15). For the oxygen mass fraction (Figure 16), it was found that oxygen is consumed throughout the combustion process, with a farther depletion distance from the burner outlet, leaving an oxygen concentration of 2.68% at the downstream end. This is comparable to the combustion of anthracite coal. The temperature distribution results (Figure 17) also show that the combustion zone shifts further from the burner. Additionally, the outer kiln surface temperature study reveals that the surface temperature in the 0–10-meter section decreases, consistent with the temperature distribution results, where the high-temperature zone moves further from the burner outlet. Around the 25-meter mark, the kiln wall temperature increases to approximately 270 °C (Figure 18).

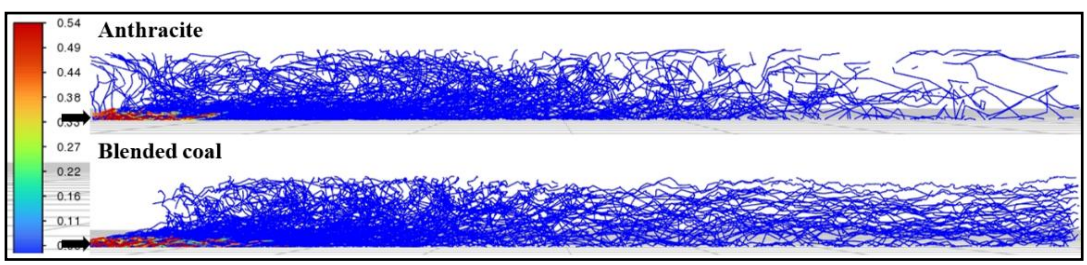

Fig. 14. Particle char mass fraction from the coal combustion model with different coal ratios

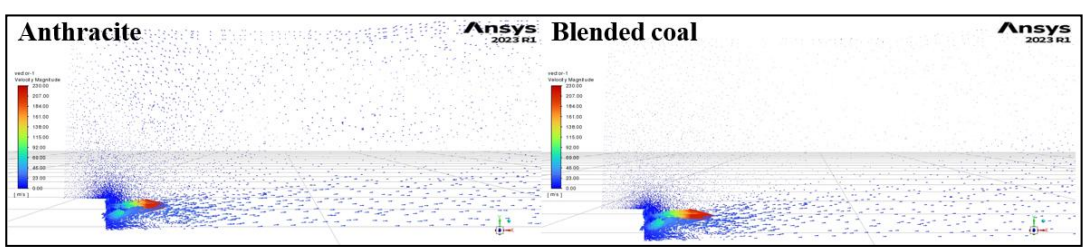

Fig. 15. Velocity vectors from the coal combustion model with different coal ratios

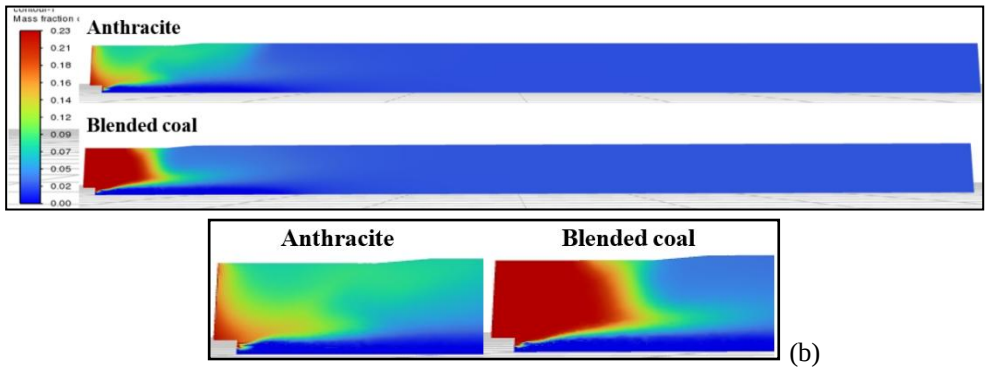

Fig. 16. Oxygen mass fraction from the coal combustion model with (a) different coal ratios and (b) near burner zone

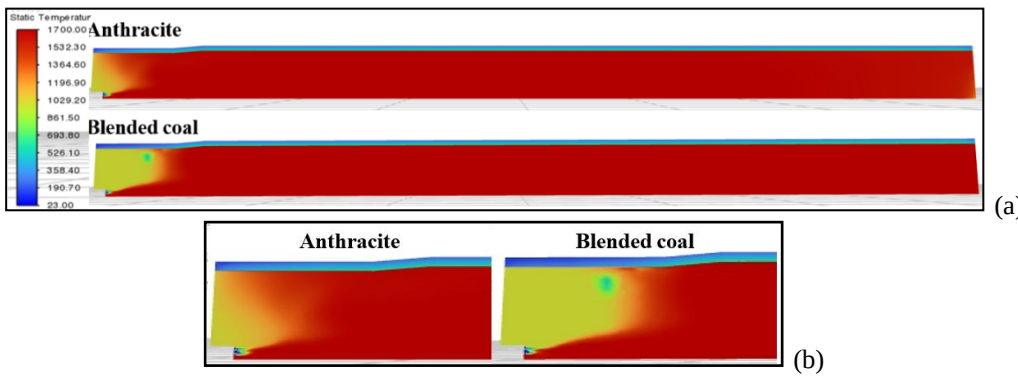

Fig. 17. Temperature distribution from the coal combustion model with (a) different coal ratios (b) near burner zone

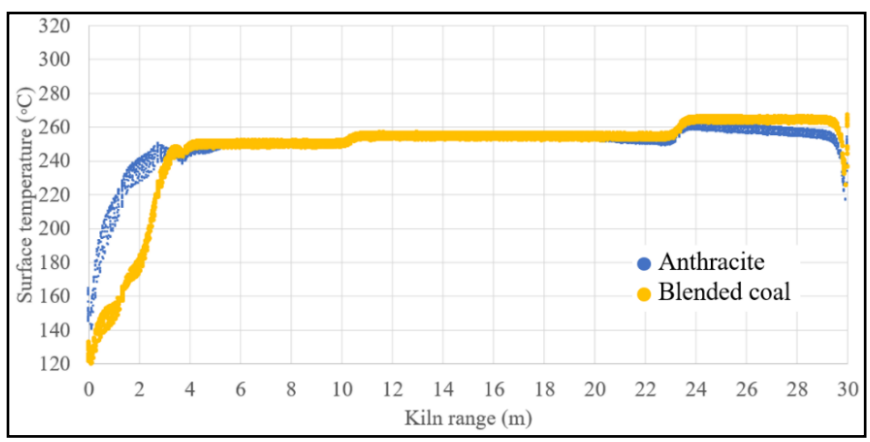

Fig. 18. Outer kiln surface temperature from the coal combustion model with different coal ratios

4.4 Simulation results of Anthracite combustion blended with petroleum coke with difference swirler angle (14°, 25° and 40°)

The simulation study found that as the swirler angle was reduced, the particle char mass fraction decreased slightly after exiting the burner outlet (Figure 19). The study of the velocity vectors at the burner outlet showed no significant changes when the swirler angle was reduced (Figure 20). Regarding the oxygen mass fraction, it was found that reducing the swirler angle resulted in similar combustion completion distances, with the oxygen concentration at the end of the model being 2.68%, 2.70% and 2.70%, respectively, for each angle (Figure 21). The temperature distribution in the kiln, based on the simulation, revealed that the zone of high combustion temperature occurred at similar distances for all swirler angles (Figure 22). The study of the outer kiln surface temperature showed that the surface temperature trends remained close throughout the model for all swirler angles (Figure 23).

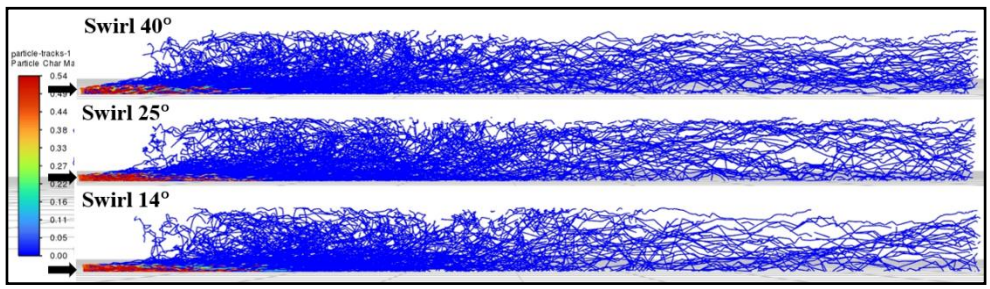

Fig. 19. Particle char mass fraction from the blended coal combustion simulation in a cement kiln with different swirl angle

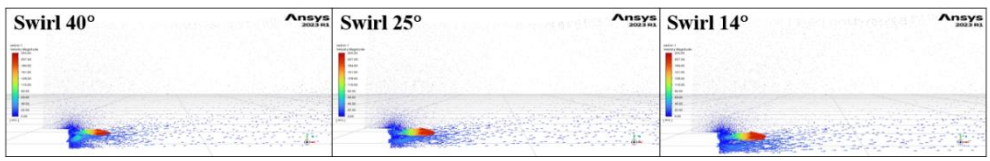

Fig. 20. Velocity vector from the blended coal combustion simulation in a cement kiln with different swirl angle

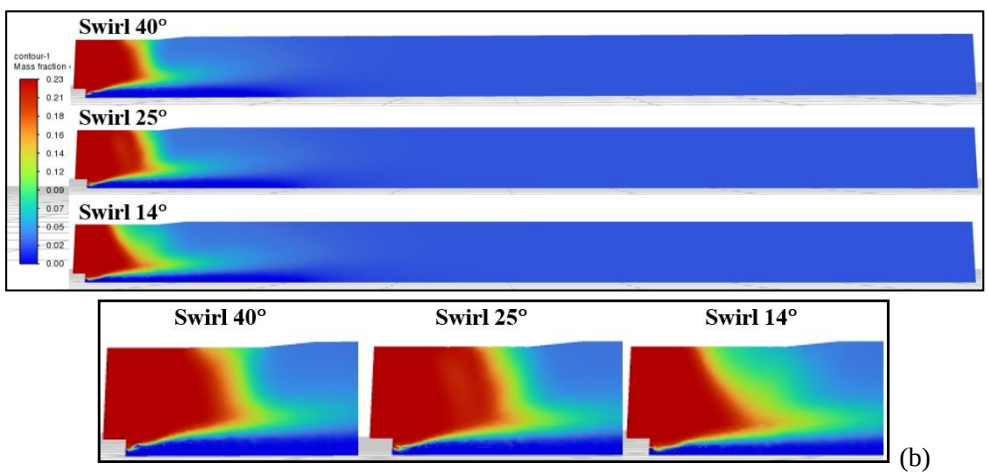

Fig. 21. Oxygen mass fraction from the blended coal combustion simulation in a cement kiln with (a) different swirl angle and (b) near burner zone

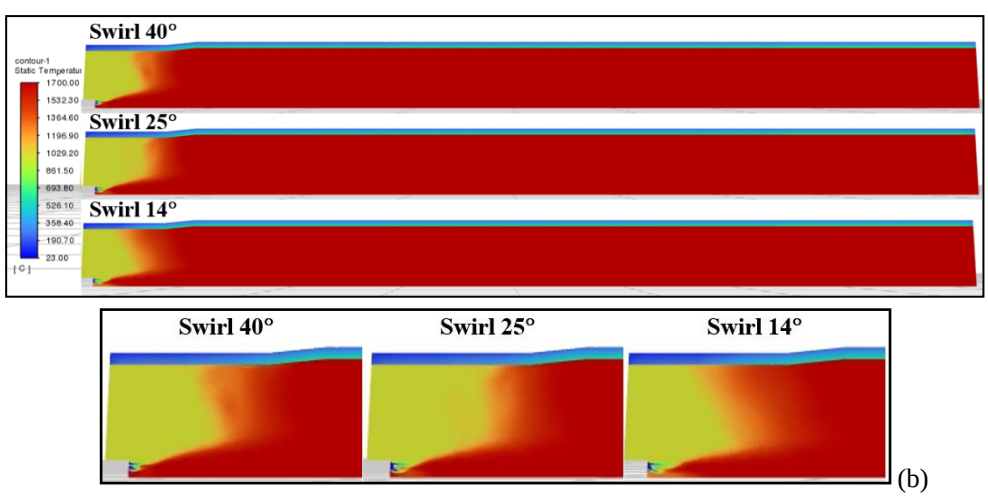

Fig. 22. Temperature distribution from the blended coal combustion simulation in a cement kiln with (a) different swirl angle and (b) near burner zone

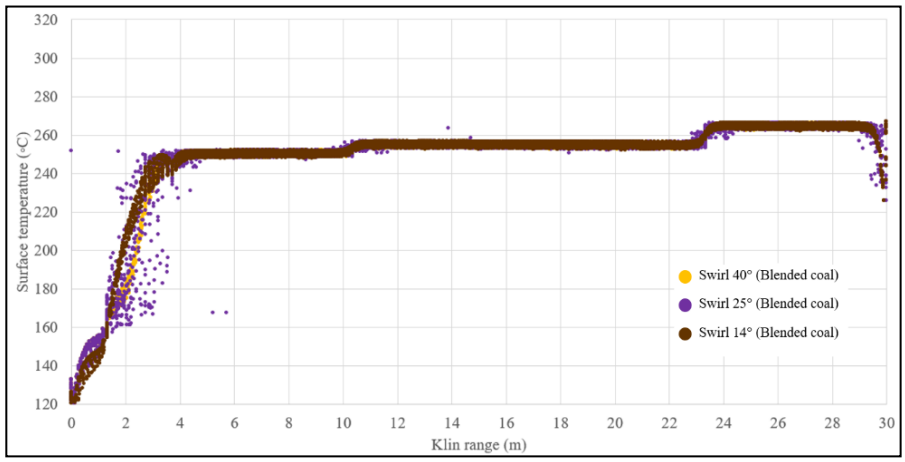

Fig. 23. Outer kiln surface temperature from the blended coal combustion simulation in a cement kiln with different swirl angle.

5. Conclusion

The research concludes that strategic adjustments to the swirler angle and the use of finely pulverized fuel blends can effectively address burner clogging issues. By shifting the combustion zone away from the burner outlet, these methods help prevent the accumulation and potential melting of coal particles, which are common contributors to blockage. Operators should consider optimizing the swirler angle as a practical approach to modifying combustion dynamics without changing the overall fuel-to-air ratio. Utilizing a blend of anthracite coal and petroleum coke with a smaller particle size can complement swirler angle adjustments by inherently improving combustion efficiency and reducing coal dispersion. Implementing these adjustments can improve the lifespan of kiln components and enhance production continuity, reducing maintenance needs and operational downtime. These findings underscore the importance of targeted mechanical and fuel composition changes to maintain efficient kiln operations and prevent issues associated with burner blockages in cement manufacturing.

Acknowledgments

This research was supported by King Mongkut's University of Technology Thonburi's Post Master Fellowship and This research project is supported by SCG Company Limited, King Mongkut's University of Technology Thonburi (KMUTT), Thailand Science Research and Innovation (TSRI), and National Science, Research and Innovation Fund (NSRF) Fiscal year 2023.

References

[1] Mastorakos E, Massias A, Tsakirogou CD, et al. CFD predictions for cement kilns including flame modelling, heat transfer and clinker chemistry. Appl Math Model. 1999;23:55–76.
[2] Wang S, Lu J, Li W, Li J, Hu Z. Modeling of pulverized coal combustion in cement rotary kiln. Energy Fuels. 2006;20(6):2350–2356.
[3] Wang M, Liao B, Liu Y, Wang S, Qing S, Zhang A. Numerical simulation of oxy-coal combustion in a rotary cement kiln. Appl Therm Eng. 2016;106:491–500.
[4] Granados D, Mejía J, Chejne F, Gomez C, Berrío A, Jurado W. Numerical simulation of oxy-fuel combustion in a cement kiln. Int Conf Energy Process Eng (ICEPE). 2011 Jun 20; Frankfurt am Main, Germany; 2011. p. 184–187.
[5] Mouratidis M, Pagoura C, Gkagkari E, et al. Coal combustion model for coupling with a cement kiln CFD model. 14th Panhellenic Chem Eng Sci Conf. 2024 May 29–31; Thessaloniki, Greece; 2024.
[6] Bhad TP, Sarkar S, Kaushik A, Herwadkar SV. CFD modeling of a cement kiln with multi-channel burner for optimization of flame profile. 7th Int Conf CFD Miner Process Ind. 2009 Dec 9–11; CSIRO, Melbourne, Australia; 2009.
[7] Mujumdar KS, Ranade VV. CFD modeling of rotary cement kilns. Asia-Pac J Chem Eng. 2008;3(2):106–118.

[8] Mikulčić H, Vujanović M, Fidaros DK, et al. The application of CFD modelling to support the reduction of CO_2 emissions in cement industry. Energy. 2012;45(1):464–473.
[9] Mikulčić H, von Berg E, Vujanović M, et al. CFD analysis of a cement calciner for a cleaner cement production. Chem Eng Trans. 2012;29.
[10] Ariyaratne WH, Malagalage A, Melaaen MC, Tokheim LA. CFD modelling of meat and bone meal combustion in a cement rotary kiln – Investigation of fuel particle size and fuel feeding position impacts. Chem Eng Sci. 2015;123:596–608.
[11] Ma AC, Zhou JM, Ou JP, Li WX. CFD prediction of physical field for multi-air channel pulverized coal burner in rotary kiln. J Cent South Univ Technol. 2006;13(1):75–79.
[12] Cecílio DM, Mateus M, Ferreiro AI. Industrial rotary kiln burner performance with 3D CFD modeling. Fuel. 2023;4(4):454–468.
[13] Alcaide-Moreno A, Castán-Lascorz MÁ, Tavares V. An industrial-scale cement rotary kiln CFD model to characterise alternative fuel combustion profiles. 36th Int Conf ECOS. 2023 Jun 25–30; Las Palmas de Gran Canaria, Spain; 2023. p. 448–459.
[14] Ngadi Z, Lahlaouti ML. CFD modeling of petcoke co-combustion in a real cement kiln: The effect of the turbulence-chemistry interaction model applied with k− ε variations. Int Rev Appl Sci Eng. 2021;13(2):148−163.
[15] Elattar HF, Specht E, Fouda A, Rubaiee S, Al-Zahrani A, Nada SA. Swirled jet flame simulation and flow visualization inside rotary kiln—CFD with PDF approach. Process. 2020;8(2):159.
[16] Elattar HF, Specht E, Fouda A, Bin-Mahfouz AS. Study of parameters influencing fluid flow and wall hot spots in rotary kilns using CFD. Can J Chem Eng. 2016;94(2):355–367.
[17] Marwan A, Thibault FG, Radi A. Experimental assessment on the coupling effect of mixing length and methane–ammonia blends on flame stability and emissions. Energies. 2023;16(7):2955.